Journal of Organometallic Chemistry 695 (2010) 2153–2159

Contents lists available at ScienceDirect

Journal of Organometallic Chemistry

journal homepage: www.elsevier.com/locate/jorganchem

Self-assembly of a novel 2D network polymer: Syntheses, characterization, crystal structure and properties of a four-tin-nuclear 36-membered diorganotin(IV) macrocyclic carboxylate

Wenjie Li, Dafeng Du, Shuangshuang Liu, Chaoguang Zhu, Adama Moussa Sakho, Dongsheng Zhu*, Lin Xu

Department of Chemistry, Northeast Normal University, 5268 Renmin Street, Changchun 130024, PR China

ARTICLE INFO

Article history:
Received 25 March 2010
Received in revised form
30 May 2010
Accepted 3 June 2010
Available online 15 June 2010

Keywords:
Self-assembly
Supramolecular chemistry
Organotin macrocycle
Naphthalene-1,4-dicarboxylic acid

ABSTRACT

The novel macrocyclic complex $(n\text{-}Bu_2SnL)_4\cdot 2C_6H_6$ **1** (LH_2 = naphthalene-1,4-dicarboxylic acid, C_6H_6 = benzene) has been synthesized by the reaction of di-n-butyltin oxide and rigid naphthalene-1,4-dicarboxylic acid. Single crystal X-ray diffraction analyse shows that complex **1** has a centrosymmetric tetranuclear diorganotin dicarboxylate with 36-membered macrocycle, which is formed by $n\text{-}Bu_2Sn$ and ligand alternately linking. All four Sn atoms are hexacoordinated, and the coordination environment can be considered as a skew-trapezoidal bipyramidal with an anisobidentate coordination mode of the carboxylate groups. Luminescent property study of complex **1** has shown that the fluorescent peak was blue-shifted and the fluorescent intensity strengthened markedly compared with ligand. Pilot studies indicated that complex **1** has shown good antitumor activities. This complex **1** is likely to serve as a new model for further investigation on the structure–antitumor activity relationship.

1. Introduction

The chemistry of organotin compounds has been studied since 1852 and developed considerably during last 30 years, highlighting the syntheses of a number of complexes with interesting properties [1–3]. Organotin carboxylates are widely used owing to their industrial and agricultural applications [4–9] as well as their potential biocidal activity [10–13]. Khan and his co-workers assumed that the organic ligand facilitates the transportation of the complexes across the cell membrane, while the antitumor activity would be wielded by the dissociated organotin(IV) moieties [12]. Recent developments in coordination chemistry have produced numerous supermolecular and macrocyclic complexes through the appropriate combination of organometallic complexes and various organic ligands [14–19]. Organotin macrocycles having large cavities or pores are attracting more and more attention for their potential applications in selective molecular recognition, storage, absorption, separation and catalysis [20–26]. So far, several di-, tri-, hexa- and octanuclear macrocyclic diorganotin carboxylates have been described [27], however, to the best of our knowledge only one literature has been repoted for a macrocyclic tetranuclear diorganotin carboxylate [28]. Worth mentioning is that [{$n\text{-}Bu_2Sn$(cis-1,4-chdca)}$_4$] contains the flexible cis-1,4-cyclohexanedicarboxylate as easy distorted ligand [28]. It has been shown that the careful selection of appropriate multidentate bridging ligands is helpful not only to obtain more novel diorganotin carboxylate macrocycles but also to realize various applications. In this work, we selected the rigid naphthalene-1,4-dicarboxylic acid(LH_2) as the ligand with the hope of constructing novel organotin(IV) coordination macrocycles with fascinating structures and/or characteristic properties. The second macrocyclic tetranuclear diorganotin carboxylate $(n\text{-}Bu_2SnL)_4\cdot 2C_6H_6$ **1** has been synthesized by the reaction of di-n-butyltin oxide and rigid naphthalene-1,4-dicarboxylic acid, and characterized by elemental analysis, IR and ^1H, ^{13}C spectroscopy, mass spectrometry and single crystal X-ray diffraction. In the molecule of complex **1**, the tin centers are coordinated to six atoms, and the coordination environment can be considered as a distorted skew-trapezoidal bipyramidal geometry. The different patterns of intermolecular weak interaction between O and Sn atoms give rise to two different types of two dimensional supramolecular macrocyclic assemblies $[(n\text{-}Bu_2SnL)_4]_n$. In addition, we found that, even though a number of organotin carboxylates have been studied before, thus, few studies have been focused on fluorimetric determination of organotin carboxylate [29]. Comparing the luminescent

* Corresponding author. Tel.: +86 13009010567.
E-mail address: zhuds206@nenu.edu.cn (D. Zhu).

0022-328X/$ – see front matter © 2010 Elsevier B.V. All rights reserved.
doi:10.1016/j.jorganchem.2010.06.001

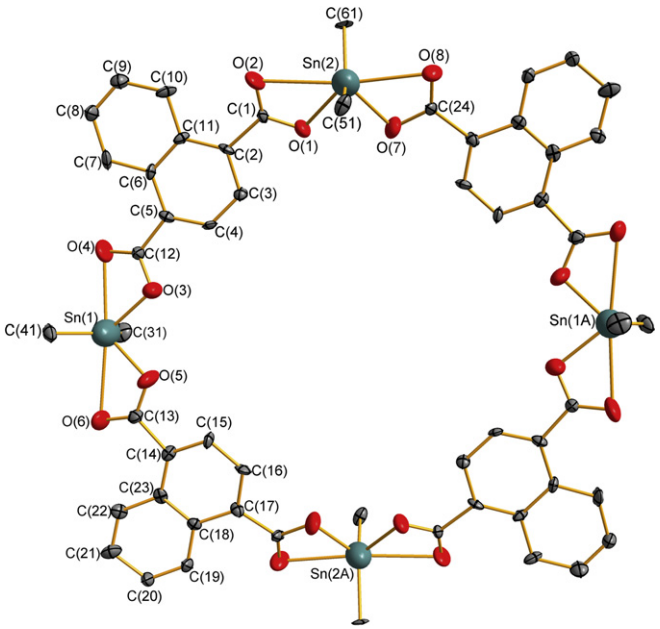

Fig. 1. The molecular structure of complex **1**. Parts of the n-butyl groups and solvent molecules have been omitted for clarity.

properties of complex **1** with ligand, we found that the fluorescent intensity of complex **1** has been strengthened markedly and the fluorescent peak blue-shifted. Furthermore, the antitumor activity of complex **1** has also been examined.

2. Results and discussion

2.1. IR spectra

The stretching frequencies of interesting are those associated with COO, Sn–O–Sn, Sn–C and Sn–O groups. The disappearance of a broad band owing to the COOH group in the region 3400–2800 cm^{-1} of ligand is indicative of the deprotonation of the carboxylic acid. The $\Delta\nu(\nu_{asCOO} - \nu_{symCOO})$ value is used to determine the nature of bonding of carboxylate to tin(IV) complexes [30]. It is generally believed that the different values in $\Delta\nu$ between asymmetric (ν_{asCOO}) and symmetric (ν_{symCOO}) absorption frequencies can distinguish the ligating mode of carboxylate moiety, that is, the value smaller than 200 cm^{-1} indicates that the carboxylate moiety is bidentate, while the value larger than 200 cm^{-1} indicates that the carboxylate moiety is unidentate. Two absorption bands were observed at 1599, 1564 cm^{-1} (ν_{asCOO}) and at 1459 and 1383 cm^{-1} (ν_{symCOO}), respectively. The $\Delta\nu(\nu_{asCOO} - \nu_{symCOO})$ values for complex **1** are 140 and 181 cm^{-1}, respectively, and indicative of bidentate chelate coordination of the caboxylate group [31,32]. This is totally consistent with the X-ray structures. A band at 615 cm^{-1} is assigned to ν(Sn–O–Sn), which indicates an Sn–O–Sn bridged structure. The absorption bands at 509 and 473 cm^{-1} are assigned to ν(Sn–C) and ν(Sn–O), respectively [33,34].

2.2. ^{1}H, ^{13}C NMR and mass spectra

The ^{1}H NMR spectrum of the complex **1** shows that the signal of the –COOH proton in the spectrum of the ligand is absent, indicating the replacement of the carboxylic acid proton by a dibutyltin moiety, and forming Sn–O bonds. The n-butyl protons show multiple resonances for the $-CH_2-CH_2-CH_2-$ skeleton in the range of 1.52–2.00 ppm and clear triplet for the terminal methyl groups at 0.93 ppm, respectively.

The ^{13}C NMR spectrum of complex **1** shows a significant downfield shift of all carbon resonances compared with the ligand; the shift is a consequence of an electron density transfer from the ligand to the metal atoms [35]. The peak at 176.90 is corresponding to the carbonyl carbon, and the carbons on naphthalene nucleus of complex **1** show multiple resonances at about 126.43–132.21 ppm. The n-butyl carbons show multiple resonances for the $-CH_2-CH_2-CH_2-$ skeleton in the range of 25.77–26.90 ppm and the terminal methyl groups at 13.60 ppm, respectively. The ^{13}C NMR spectroscopic data for complex **1** are consistent with organotin carboxylate structure.

The molecular weight determination is rather difficult for organotin complexes containing multiple tin atoms because of the extensive number of unusual molecular adducts [36]. The molecular ion is not observed but the fragment ions found are in agreement with the structure of complex **1**. The mass spectra of complex **1** reveals structurally important fragment ions at m/z 233 $[n\text{-}Bu_2Sn]^+$ and m/z 319 $[n\text{-}Bu_2Sn(COO)_2]^+$, at the same time, peaks for tetrameric ($m/z = 1788$), trimeric ($m/z = 1341$), dimeric ($m/z = 894$) and monomeric ($m/z = 447$) species are observed in the mass spectrum.

2.3. Crystal structure

Complex **1** was synthesized by azeotropic removal of water from the reaction in dried benzene between the di-n-butyl oxide and

Table 1
Selected bond lengths (Å) and bond angles (deg) for **1**.

Bond lengths	Sn1	Sn2		Sn1	Sn2
Sn–Ocov	2.069(5)	2.115(5)	C–Ocov	1.307(8)	1.290(8)
	2.087(5)	2.120(7)		1.309(8)	1.305(8)
Sn···Ocoord	2.593(6)	2.561(5)	C–Ocoord	1.220(8)	1.236(8)
	2.754(6)	2.667(5)		1.222(8)	1.246(8)
Sn–C	2.103(8)	2.102(7)	Sn···O′intermol	3.277	3.230
	2.109(7)	2.120(7)			
Bond angles	**Sn1**	**Sn2**		**Sn1**	**Sn2**
C–Sn–C	142.0(3)	142.4(3)	Ocov–Sn–C	102.6(3)	101.1(2)
Ocov–Sn–Ocov	81.18(19)	82.30(17)		104.7(3)	102.0(2)
Ocov–Sn–Ocoord	51.88(19)	53.14(18)		104.3(3)	105.0(2)
	54.55(19)	55.22(18)		105.5(3)	108.0(2)
Ocoord–Sn–Ocoord	172.1 (2)	169.2(2)	Sn–Ocov–C	103.3(4)	102.5(4)
Ocoord–Sn–O′intermol	70.05	67.56		108.7(4)	105.2(4)
Sn–O–Sn′	109.95	112.44	Sn–Ocoord–C	78.5(4)	80.6 (4)
O–C–O	120.2(7)	119.1(6)		81.9 (4)	82.9 (4)
	120.6(6)	120.6(6)			

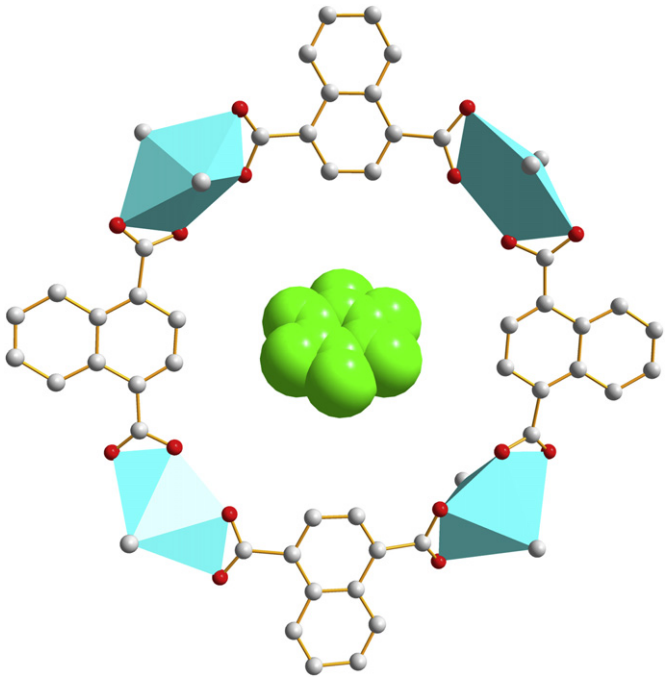

Fig. 2. Fragment of the crystal lattice of complex **1**, showing the inclusion of aromatic ring within the macrocycle void.

naphthalene-1,4-dicarboxylic acid in the 1:1 molar ratio, and filtrated to get clear solution, then the filtrate was allowed to slow evaporation of benzene at room temperature to give crystals suitable for X-ray diffraction analysis.

The molecular structure of complex **1** is shown in Fig. 1; selected bond lengths and bond angles are listed in Table 1.One macrocycle and two solvent benzene molecules are included in the independent crystal cell. In the molecular structure of complex **1**, n-Bu_2Sn and ligand alternately link into a four-tin-nuclear 36-membered diorganotin(IV) macrocycle. Each tin atom is hexacoordinated and the coordination configuration can be described as a skewed-trapezoidal bipyramidal geometry with four oxygen atoms of the two carboxylate moieties occupying the equatorial positions and the axial positions occupied by the n-butyl groups [37]. The shorter of the Sn–O bonds being ≤2.2 Å and the longer Sn–O bonds being ≥2.5 Å, indicated asymmetrically coordinated carboxylate oxygen atoms, and the two organo substituents disposed over the longer Sn–O vectors with C–Sn–C angles in the range 130–150° [38]. Due to the anisobidentate coordination mode of the carboxylate groups to the tin atoms, two groups of different Sn–O bond lengths were found, one group corresponding to Sn–O bonds of covalent character, 2.069(5)–2.120(7) Å, and the other group corresponding to Sn–O bonds of coordinative character, 2.561(5)–2.754(6) Å and the C–Sn–C bond angles of 142.0(3)–142.4(3)°. The geometry of the tin centers in complex **1** conforms to the common structural motif found for compounds with the general formula [$R_2Sn(O_2CR')_2$].

As shown in Fig. 2, the width of the macrocycle is 15.51 × 14.79 Å [Sn(1)···Sn(1A) and Sn(2)···Sn(2A)], which is larger than those in di-n-butyltin(IV) cis-1,4-cyclohexanedicarboxylate [28]. The macrocyclic voids of complex **1** allow for the inclusion of two benzene molecules, which in the solid-state structure are accomodated above and below the molecule center. For clarity, the aromatic guest molecule is uniformly colored (dark green). The framework connectivity of complex **1** with the tin coordination sphere is shown as blue skewed-trapezoidal bipyramidal.

Interestingly, from the X-ray structure, it can be divided into two distinct one-dimensional chains resulting from the different weak intermolecular interactions. The tetranuclear macrocyclic rings in the crystal lattice are linked into polymeric chains along axis *b* through an extensive set of weak intermolecular Sn(1)···O(6) (Fig. 3) [39–44], in which all tin atoms and carboxylate groups are included. Besides these weak intermolecular Sn(2)···O(2), C(51)–H(51B)···O(2) interactions [45–47] are also involved for linking the molecules into a one-dimensional polymeric structure with extended zigzag chains running parallel to the crystallographic *c*-axis (Fig. 4). The hydrogen atoms involved in the C–H···O interactions [H(51B)] belong to the n-butyl moiety, while the oxygen atoms are derived from the carboxylate [O(2)]. The distance of the C–H···O interactions is H(51B)···O(2) 2.551 Å. These Sn···O interactions vary from 3.230 to 3.277 Å [Sn(2)···O(2) and Sn(1)···O(6)] which are longer than the reported Sn···O interactions [2.968(6)–3.208(6) Å] [27], being significantly shorter than the sum of the van der Waals radii for tin and oxygen atoms (3.70 Å) [48], therefore these oxygen atoms can be considered as bonding. The geometry found about the tin atom in the complex **1** is best described as a skew-trapezoidal bipyramid geometry and closely resembles those found for the structures of n-Bu_2Sn-$(O_2CCH_2SC_6H_5)_2$ [49], n-$Bu_2Sn[O_2CC_5H_3N(SMe\text{-}2)]_2$ [50], n-Bu_2Sn-$[O_2CC_6H_3(OH)_2$ 2,4$]_2$ [51], and n-$Bu_2Sn(O_2CC_4H_4NOS_2)_2$ [52].

These Sn···O interactions give rise to the formation of two kinds of Sn_2O_2 [Sn(2A)···O(2A)···Sn(2B)···O(2B) and Sn(1A)···O(6A)···Sn(1B)···O(6B)] distannoxane units which are highly distorted as evidenced by the difference in the O···Sn···O bond angles, 70.05° for Sn(1) and 67.56° for Sn(2), and Sn···O···Sn bond angles, 109.95–112.44°. Considering the Sn···O interactions, the coordination environment of all tin atoms can be described also as distorted bipyramidal-pentagonal. The infinite chains are interlocked between each other by alternate threading of Sn-n-butyl groups of one chain through the macrocyclic cavities of two neighboring chains. Therefore, self-assembly occurs through an extensive set of intermolecular Sn···O, C–H···O interactions and helps the molecules form a 2D architecture with another type of tetranuclear macrocycle (**II**) having larger cavity (Fig. 5). The width of the cavity can be evaluated by the transannular Sn···Sn distance, which is 15.49 × 16.86 Å [Sn(1A)···Sn(1C) and Sn(2B)···Sn(1D)].

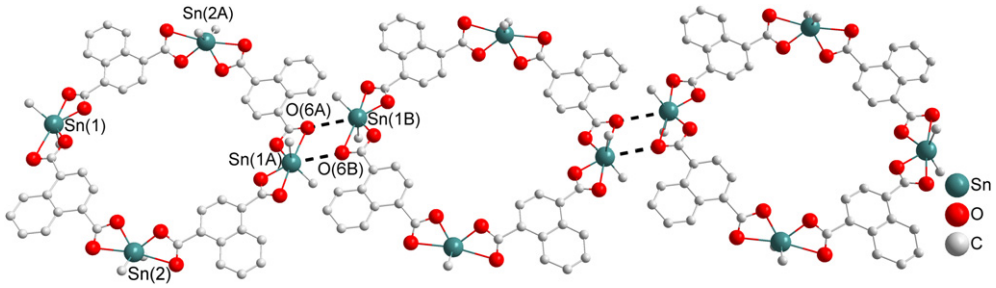

Fig. 3. The 1D infinite polymeric chain structure of complex **1** along axis *b* formed through intermolecular Sn···O interactions. Parts of the n-butyl groups and solvent molecules been omitted for clarity.

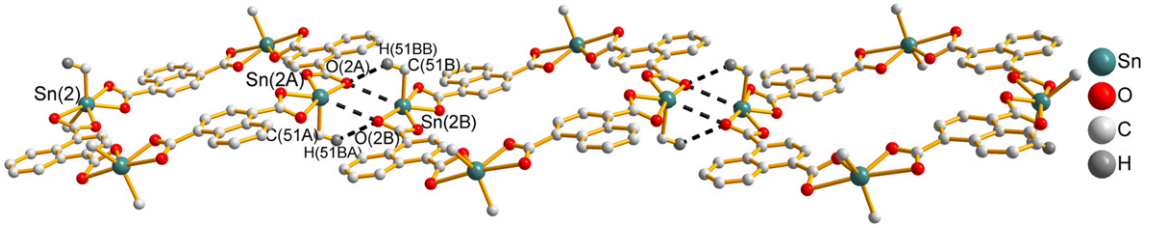

Fig. 4. Polymeric zigzag chains along axis *c* formed through intermolecular Sn···O and C–H···O interactions between the macrocyclic tetranuclear complexes present in the crystal lattice of complex **1**.

2.4. Luminescent property

The luminescent properties of the organotin(IV) complex **1** and naphthalene-1,4-dicarboxylic acid in the solid state have been investigated with a 150 W xenon lamp as the excitation source. Emission spectra of complex **1** and ligand are shown in Fig. 6. An emission peak at ca. 483 nm was observed in ligand, and complex **1** was blue-shifted up to about 459 nm and the fluorescent intensity strengthened markedly. Complex **1** showed bright blue (ca. 459 nm) emission when illuminated by UV-light of 350 nm.

The luminescence lifetimes were calculated to be 9 and 22 ns for complex **1** and ligand, respectively, which are also showed in Fig. 7 and Fig. 8. The luminescence lifetime of complex **1** and ligand are much shorter than the lifetime of the emission resulted from a triplet state ($>10^{-3}$ s), so the emissions of complex **1** should arise from a singlet state [53]. Furthermore, the absolute emission quantum yields estimated for complex **1** and ligand are 47.4% and 13.3%, respectively. The results showed that, compared to the ligand, complex **1** exhibits a stronger emission, higher quantum yield. However, the effect of the microenvironment between the ligand and complex **1** on the luminescence properties still needs further fundamental investigations.

2.5. Antitumor activity

We examined the antitumor activity of complex **1** against collection of HeLa, HT1080, U87 cell lines. MTT assay was used with a relative short exposure (24 h) to the test complex **1** (10 μg/mL) (Fig. 9). In Fig. 9, we can see that the growth inhibition of HeLa cells to 10 μg/mL solutions of complex **1** is best. Fig. 10 depicts antitumor effects against three cancer cell lines by different concentrations (0.3, 1, 3, 10, and 30 μg/mL) of complex **1**. The results showed that the susceptibilities to destruction vary with both the nature of complex **1** and the type of cancer cells. Fig. 10 strikingly depicts the concentration-dependent decrease and the inhibition values tended to converge at the highest dose. These aspects are examined for each cell line and the five concentrations on the basis of the data listed in the Fig. 10. The derived IC_{50} values are listed in Table 2.

Crowe and his co-workers assumed that organotin complexes anticancer mechanism is that active ion $R_nSn^{(4-n)+}$ forms by hydrolysis of the complexes, then directly combine to DNA base; And before the formation of Sn–DNA, dissociation of organotin complexes may be a critical step, organic acid ligand plays an important role in the transportation of the organotin complexes to the appropriate location, then organotin complexes through hydrolysis slowly releases $R_nSn^{(4-n)+}$. Complexes are too lively or too stable for hydrolysis to cause the activity decreased; In other words, the more lively or stable complexes have lower activities [54]. Atassi et al. also said, majority of organotin drug, which had been determined its antitumor activity, are poorly soluble in water, this may be a major obstacle to improve the anticancer activity of organotin drug.

In our work, to test whether the effect of the Sn(IV) complex **1** could be attributed to dicarboxylic acid ligand alone or not, we tested the effect of ligand alone against each cell line. The ligand exhibited almost no inhibition of cellular proliferation ($IC_{50} > 300$ μg/mL, data

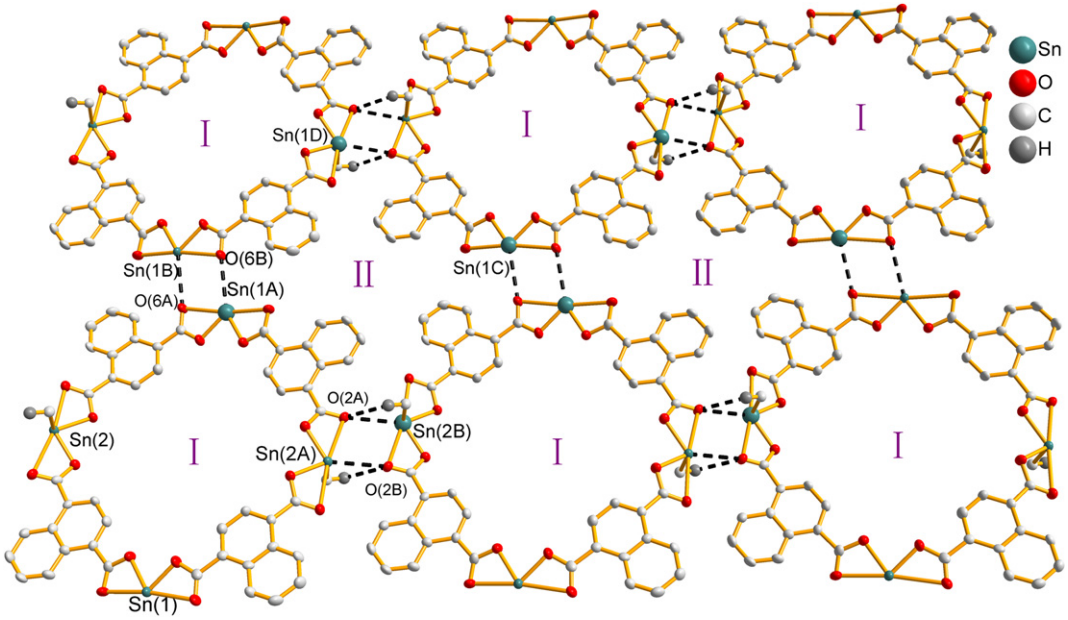

Fig. 5. Two dimensional supramolecular assembly of complex **1** formed from intermolecular Sn···O, C–H···O interactions.

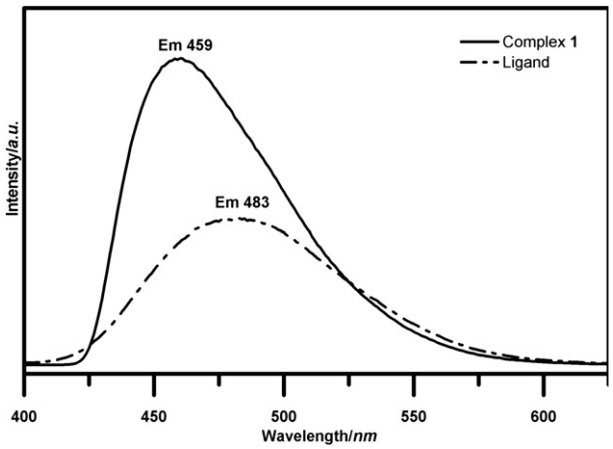

Fig. 6. Emission spectra of complex **1** and ligand.

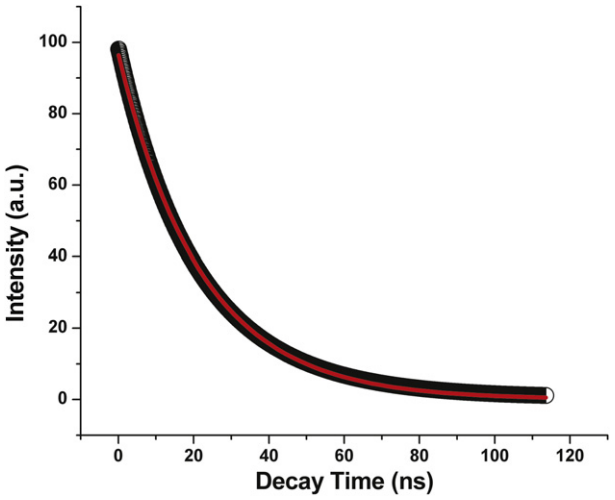

Fig. 8. Luminescence decay curve for ligand.

not shown). The results showed that the antitumor activity of complex **1** is rather promising than ligand LH_2. From the derived IC_{50} values it is concluded that the activity of complex **1** against HeLa cells is better than against HT1080 and U87 cell lines. It is noteworthy that complex **1** has a better antitumor activity against the three cell lines than the corresponding ligand LH_2, which have shown that the complex **1** exhibited good antitumor activities and have a potential to be used as drug. Fat-solubility of di-n-butyltin oxide is poor and it is not easy to be hydrolyzed into active ion ($n\text{-}Bu_2Sn^{2+}$), while organic acid ligand enhances organotin carboxylate's fat-solubility and the L (RCOO) plays an important role after hydrolysis for the transportation of the organotin(IV) moiety to an action site [11,12,55]. As these results are preliminary, further study on the antitumor effects of complex **1** is highly recommended.

3. Experimental section

3.1. General and instrumental

The melting point was obtained with Kofler micro-melting point apparatus and are uncorrected. Elemental analyses (C, H) were carried out on a Perkin–Elmer PE 2400 CHN instrument and by gravimetric analysis for Sn. ^1H, ^{13}C NMR spectra was recorded in $CDCl_3$ on a Varian Mercury 300 MHz spectrometer. IR spectra (KBr pellets) were recorded on an Alpha Centauri FI/IR spectrometer (400–4000 cm^{-1} range). The photoluminescence spectra were recorded on a Hitachi F-4500 fluorescence spectrophotometer equipped with xenon lamp as excitation source. Luminescence lifetime was obtained with a FluoroLog-3 (Horiba Jobin Yvon) spectrometer, quantum yield at room temperature was measured using an absolute PL quantum yield measurement system (C9920-02, Hamamatsu photonics k.k.). The ion source Fourier transform mass spectrometers was used for this study. The instrument, a HiResMALDI FTMS made by IonSpec Corp. (Irvine, CA), is equipped with a 4.7-T superconducting magnet. The use a rf-only quadrupole ion guide to transport ions from the external ion source to the FTMS analyzer. The instrument also has an OMEGA data system made by IonSpec Corp. for controlling the instrument parameters and analyzing the Fourier transform signals.

The [3-(4,5-dimethylthiazol-2-yl)-2,5-diphenyl tetrazolium bromide] (MTT) assay that differentiates dead from living cells was adapted [56–59]. Dissolved MTT is converted to an insoluble purple formazan by cleavage of the tetrazolium ring induced by dehydrogenase enzymes present in viable cells. Dead cells do not cause this change. The following reagents and instruments were used: MTT reagent, 5 mg/mL in phosphate buffered saline, protected from light, and stored at −20 °C; microplate reader (Bio-Rad Co., Hercules, CA).

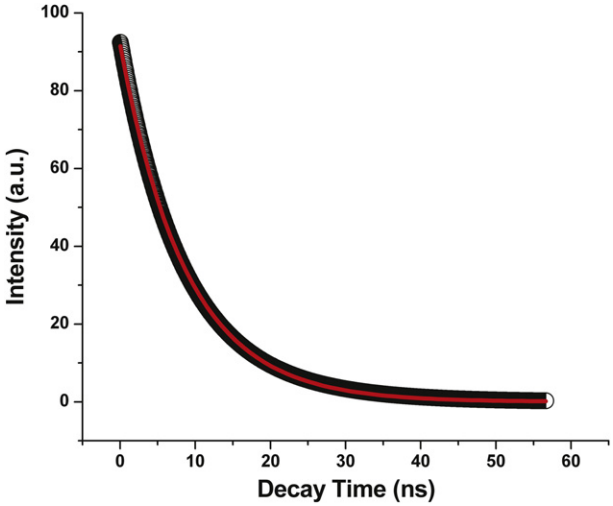

Fig. 7. Luminescence decay curve for complex **1**.

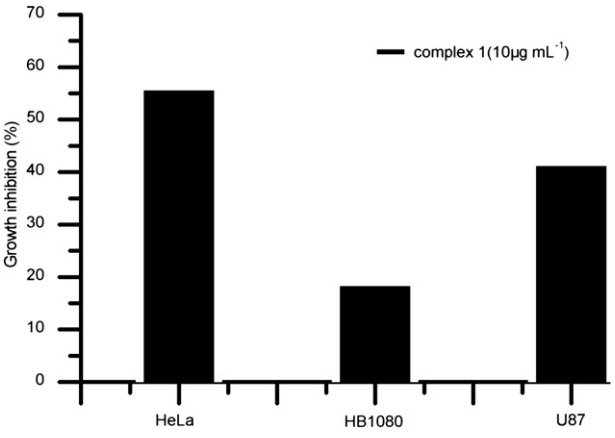

Fig. 9. Antitumor effects against HeLa cancer cells, HT1080 cancer cells, and U87 cancer cells. Each exposed to 10 μg/mL solutions of complex **1**.

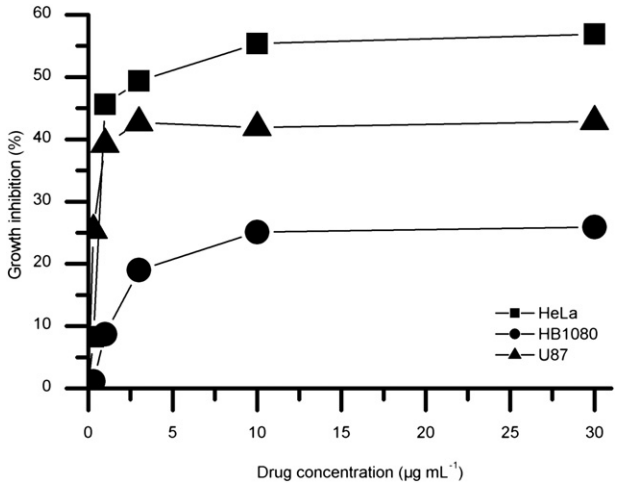

Fig. 10. Antitumor effects against HeLa cancer cells, HT1080 cancer cells, and U87 cancer cells. Each exposed to 0.3,1,3, 10, and 30 μg/mL solutions of complex **1**.

The assay was carried out as follows: cell lines were seeded into a 96-well microplate (about 1×10^4 cells/well) and incubated for 24 h. The dosage level of the test compounds on the selected cell lines was 10 μg/ml. After 24 h of incubation at 37 °C, the MTT (final concentration = 0.5 mg/mL) was added to each well. After 4 h of incubation at 37 °C, then 200 uL of DMSO was added to each well. The optical density (OD) was then read at a wavelength of 570 nm. The decrease in OD measures the extent of decrease in the number of cancer cells exposed to the test compounds.

Di-n-butyltin oxide, naphthalene-1,4-dicarboxylic acid were purchased from Aldrich and used without further purification. Tumor cell lines adopted for this study were HeLa (cervical), HT1080 (fibrosarcoma), U87 (glioma). They were bought from ATCC (American Type Cultire Collection). These human cells were cultured as monolayers in RPMI 1640 medium supplemented with 10% fetal bovine serum(GIBCO), 100 U/mL penicillin, and 100 mg/mL streptomycin. Cell culture reagents were obtained from GibcoBRL (Life Technologies, Cergy-Pontoise, France). Each sample was dissolved in DMSO and stored at 4 °C. Antiproliferative effects were not seen at a concentration of 0.01% of dimethylsulfoxide.

3.2. X-ray crystallography

Diffraction intensities for complex **1** were collected on a Bruker CCD Area Detector image plate diffractometer by using the ω/φ scan technique with Mo-Kα radiation ($\lambda = 0.71073$ Å). Absorption corrections were applied by using multiscan techniques [60]. The structure was solved by direct methods with SHELXS-97 [61] and refined using SHELXL-97 [62]. All non-hydrogen atoms were refined with anisotropic temperature parameters; hydrogen atoms were refined as rigid groups. Crystallographic data for structural analysis have been deposited with the Cambridge Crystallographic Data Center, CCDC 708347 for complex **1**. Crystal data and refinement results for complex **1** are collated in Table 3.

Table 2
Concentration of complex **1** to obtain 50% inhibition of HeLa, HT1080, U87 proliferative activity.

	IC50		
Drug labeling	HeLa	HT1080	U87
Complex **1**	6.558	177.257	82.732

Table 3
Crystal data and details of structure refinement parameters for complex **1**.

Empirical formula	$C_{92}H_{108}O_{16}Sn_4$
Formula weight	1944.54
Temperature	273(2) K
Wavelength	0.71073 Å
Crystal system, space group	Triclinic, *P*-1
Unit cell dimensions	$a = 9.9206(10)$Å; alpha = 108.643(2)°
	$b = 12.8928(13)$Å; beta = 93.764(2)°
	$c = 18.3611(18)$Å; gamma = 102.942(2)°
Volume	2144.6(4) Å^3
Z, Calculated density	1, 1.506 Mg/m^3
Absorption coefficient	1.216 mm^{-1}
F(000)	988
Crystal size	0.37 × 0.33 × 0.28 mm
Theta range for data collection	1.72–26.05°
Limiting indices	$-12 \le h \le 12$, $-15 \le k \le 15$, $-22 \le l \le 18$
Reflections collected/unique	12156/8277 [R(int) = 0.0404]
Completeness to theta = 26.05	97.6%
Refinement method	Full-matrix least-squares on F^2
Data/restraints/parameters	8277/22/523
Goodness-of-fit on F^2	0.954
Final *R* indices [$I > 2$sigma(I)]	$R_1 = 0.0573$, $wR_2 = 0.1111$
R indices (all data)	$R_1 = 0.1090$, $wR_2 = 0.1308$
Largest diff. peak and hole	1.123 and −0.605 e Å^{-3}

3.3. Syntheses

Di-n-butyltin oxide (0.248 g, 1.0 mmol) and naphthalene-1,4-dicarboxylic acid (0.216 g, 1.0 mmol) were added into dried benzene (50 mL) and refluxed for 6 h. A Dean–Stark apparatus was used to facilitate the dynamic removal of the water formed in the reaction by azeotropic distillation. After cooled to room temperature, the reaction mixture was filtrated. The filtrate was allowed to slow evaporation of benzene at room temperature to afford colourless crystals of complex **1** (0.369 g, 76%). mp 220–222 °C. (Found: C 56.78; H 5.65; Sn 24.45%. $C_{92}H_{108}O_{16}Sn_4$ requires C 56.82; H 5.60; Sn 24.42%.) νmax (KBr)/cm^{-1} 1599, 1564, 1459, 1383, 615, 509, 473. ^{1}H NMR (300 MHz, $CDCl_3$, 20 °C, TMS): $\delta = 0.93$ (t, 6 H, Hδ), 1.52 (tq, 4 H, Hγ), 1.89 (m, 4 H, Hβ), 2.00 (m, 4 H, Hα), 7.71 (t, 2 H, H7, H8), 8.54 (s, 2 H, H2, H3), 9.16 (t, 2 H, H6, H9) ppm. ^{13}C NMR ($CDCl_3$): $\delta = 13.60$ (C-δ), 26.38 (C-γ), 26.90 (C-β), 25.77 (C-α), 131.32 (C1, C4), 130.11 (C2, C3), 132.21 (C5, C10), 127.78 (C6, C9), 126.43 (C7, C8), 176.90 (COO) ppm. MS: $m/z(\%) = 233$ (42) [n-Bu_2Sn]$^+$, 319 (15) [n-$Bu_2Sn(COO)_2$]$^+$, 449 (21) [$M_{monomer} + 2H$]$^+$, 917 (10) [$M_{dimer} + Na$]$^+$, 1356 (9) [$M_{trimer} + Me$]$^+$, 1753 (6) [$M_{tetramer}$ − n-Bu+Na]$^+$.

4. Conclusion

In conclusion, this contribution has shown that the combination of a dibutyltin(IV) moiety with an aromatic dicarboxylate results in the formation of complex with a tetranuclear macrocyclic molecular structure. Interestingly, the macrocyclic cavity of complex **1** is large enough for the introduction of two benzene molecules. In light of the above results, It is worthy to note that, the formation of two kinds of Sn_2O_2 distannoxane units through the Sn···O interactions, which probably play an important role in the formation of two distinct one-dimensional chains and a 2D polymeric network structure. Further, intermolecular hydrogen bonds of C–H···O interactions stabilize the structure. In addition, the luminescent property results showed that, compared to the ligand, complex **1** exhibits a stronger emission, higher quantum yield. From the derived IC_{50} values it is concluded that the sequence or activity against complex **1** is: HeLa > U87 > HT1080.

Acknowledgments

We acknowledged the Postdoctoral Science Foundation PR China (No. 2005038561).

Supplementary material

CCDC 708347 contains the supplementary crystallographic data (complex **1**) for this paper. These data can be obtained free of charge from The Cambridge Crystallographic Data Centre via http://www.ccdc.cam.ac.uk/data_request/cif.

References

[1] J. Beckmann, K. Jurkschat, Chem. Rev. 215 (2001) 267–300.
[2] L. Pellerito, L. Nagy, Coord. Chem. Rev. 224 (2002) 111–150.
[3] M.J. Clarke, F.C. Zhu, D.R. Frasca, Chem. Rev. 99 (1999) 2511–2534.
[4] H.D. Yin, G. Li, Z.J. Gao, H.L. Xu, J. Organomet. Chem. 691 (2006) 1235–1241.
[5] M.I. Khan, M.K. Baloch, M. Ashfaq, J. Organoment. Chem. 689 (2004) 4584–4591.
[6] I.W. Nowell, J.S. Brooks, G. Beech, R. Hill, J. Organomet. Chem. 244 (1983) 119–124.
[7] G.K. Sandhu, R. Gupta, S.S. Sandhu, R.V. Parish, Polyhedron 4 (1985) 81–87.
[8] G.K. Sandhu, R. Gupta, S.S. Sandhu, R.V. Parish, K. Brown, J. Organomet. Chem. 279 (1985) 373–384.
[9] T.P. Lochhart, F. Davidson, Organometallics 6 (1987) 2471–2478.
[10] K.C. Molloy, T.G. Purcell, E. Hahn, H. Schumann, J.J. Zuckerman, Organometallics 5 (1986) 85–89.
[11] M. Ashfaq, M.I. Khan, M.K. Baloch, A. Malik, J. Organomet. Chem. 689 (2004) 238–245.
[12] M.I. Khan, M.K. Baloch, M. Ashfaq, J. Organomet. Chem. 689 (2004) 3370–3378.
[13] M.I. Khan, M.K. Baloch, M. Ashfaq, G. Stoter, J. Organomet. Chem. 691 (2006) 2554–2562.
[14] M. Eshel, A. Bino, Inorg. Chim. Acta 320 (2001) 127–132.
[15] O.I. Shchegolikhina, V.A. Igonin, Yu. A. Molodtsova, Yu. A. Pozdniakova, A. A. Zhdanov, T.V. Strelkova, S.V. Lindeman, J. Organomet. Chem. 562 (1998) 141–151.
[16] E. Kiss, K. Petrohan, D. Sanna, E. Garribba, G. Micera, T. Kiss, Polyhedron 19 (2000) 55–61.
[17] D. Dakternieks, A. Duthie, B. Zobel, K. Jurkschat, M. Schürmann, E.R.T. Tiekink, Organometallics 21 (2002) 647–652.
[18] S. Bhandari, M.F. Mahon, J.G. McGinley, K.C. Molloy, C.E.E. Roper, J. Chem. Soc., Dalton Trans. (1998) 3425–3430.
[19] M. Verdenelli, S. Parola, L.G. Hubert-Pfalzgraf, S. Lecocq, Polyhedron 19 (2000) 2069–2075.
[20] C.N.R. Rao, S. Natarajan, R. Vaidhyanathan, Angew. Chem., Int. Ed. 43 (2004) 1466–1496.
[21] F. Würthner, C.C. You, C.R. Saha-Möller, Chem. Soc. Rev. 33 (2004) 133–146.
[22] M.W. Hosseini, Acc. Chem. Res. 38 (2005) 313–323.
[23] J.L.C. Rowsell, O.M. Yaghi, Angew. Chem., Int. Ed. 44 (2005) 4670–4679.
[24] J.R. Nitschke, Acc. Chem. Res. 40 (2007) 103–112.
[25] M.A. Pitt, D.W. Johnson, Chem. Soc. Rev. 36 (2007) 1441–1453.
[26] J.A. Thomas, Chem. Soc. Rev. 36 (2007) 856–868.
[27] A. Davies, M. Gielen, K. Panell, E. Tiekink, H. Höpfl, Tin Chemistry: Fundamentals, Frontiers and Applications. Wiley-VCH, Weinheim, 2008.
[28] I.F. Hernández-Ahuactzi, J. Cruz-Huerta, V. Barba, H. Höpfl, L.S. Zamudio-Rivera, H.I. Beltrán, Eur. J. Inorg. Chem. (2008) 1200–1204.
[29] L. Pellerito, A. Pellerito, F. Maggio, M. Beltramini, B. Salvato, F. Ricchelli, Appl. Organomet. Chem. 7 (1993) 79–84.
[30] V. Chandrasekhar, V. Bhaskar, A. Steiner, S. Zacchini, Organometallics 21 (2002) 4528–4532.
[31] H.D. Yin, C.H. Wang, Q.J. Xing, Polyhedron 23 (2004) 1805–1810.
[32] D. Kovala-Demertzi, N. Kourkoumelis, A. Koutsodimou, A. Moukarika, E. Horn, E.R.T. Tiekink, J. Organomet. Chem. 620 (2001) 194–201.
[33] G.K. Sandhu, N. Sharma, E.R.T. Tiekink, J. Organomet.Chem. 403 (1991) 119–131.
[34] D. Kovala-Demertzi, V.N. Dokorou, J.P. Jasinski, A. Opolski, J. Wiecek, M. Zervou, M.A. Demertzis, J. Organomet. Chem. 690 (2005) 1800–1806.
[35] C.L. Ma, Q.F. Wang, R.F. Zhang, Inorg. Chem. 47 (2008) 7060–7061.
[36] T.S. Basu Baul, W. Rynjah, E. Rivarola, A. Lyčka, M. Holčapek, R. Jirásko, D. de Vos, R.J. Butcher, A. Linden, J. Organomet. Chem. 691 (2006) 4850–4862.
[37] S.G. Teoh, S.H. Ang, E.S. Looi, S.B. Keok, J.P. Teo, J.P. Declercq, J. Organomet. Chem. 523 (1996) 75–78.
[38] S.P. Narula, S.K. Bharadwaj, H.K. Sharma, Y. Sharda, G. Mairesse, J. Organomet. Chem. 415 (1991) 203–209.
[39] V. Chandrasekhar, S. Nagendran, V. Baskar, Coord. Chem. Rev. 235 (2002) 1–52.
[40] H.I. Beltrán, L.S. Zamudio-Rivera, T. Mancilla, R. Santillan, N. Farfan, Chem.—Eur. J. 9 (2003) 2291–2306.
[41] R. Garcia-Zarracino, J. Ramos-Quiñones, H. Höpfl, Inorg. Chem. 42 (2003) 3835–3845.
[42] R. Garcia-Zarracino, H. Höpfl, Angew. Chem., Int. Ed. 43 (2004) 1507–1511.
[43] L.S. Zamudio-Rivera, R. George-Tellez, G. Lopez-Mendoza, A. Morales-Pacheco, E. Flores, H. Höpfl, V. Barba, F.J. Fernandez, N. Cabirol, H.I. Beltran, Inorg. Chem. 44 (2005) 5370–5378.
[44] R. Garcia-Zarracino, H. Höpfl, J. Am. Chem. Soc. 127 (2005) 3120–3130.
[45] V. Chandrasekhar, P. Singh, K. Gopal, Organometallics 26 (2007) 2833–2839.
[46] V. Chandrasekhar, K. Gopal, S. Nagendran, P. Singh, A. Steiner, S. Zacchini, J.F. Bickley, Chem.—Eur. J. 11 (2005) 5437–5448.
[47] T. Steiner, B. Lutz, J. van der Maas, A.M.M. Schreurs, J. Kroon, M. Tamm, Chem. Commun. (1998) 171–172.
[48] R.G. Swisher, J.F. Vollano, V. Chandrasekhar, R.O. Day, Inorg. Chem. 23 (1984) 3147–3152.
[49] G.K. Sandhu, N. Sharma, E.R.T. Tiekink, J. Organomet. Chem. 371 (1989) C1–C3.
[50] M. Gielen, A.E. Khloufi, M. Biesemans, R. Willem, Polyhedron 11 (1992) 1861–1868.
[51] S.G. Teoh, S.H. Ang, J.P. Declercq, Polyhedron 16 (1997) 3729–3733.
[52] R.F. Zhang, J.F. Sun, C.L. Ma, J. Organomet. Chem. 690 (2005) 4366–4372.
[53] J.F. Ma, J. Yang, S.L. Li, S.Y. Song, H.J. Zhang, H.S. Wang, K.Y. Yang, Cryst. Growth Des. 5 (2005) 807–812.
[54] A.J. Crowe, P.J. Smith, G. Atassi, Inorg. Chim. Acta 93 (1984) 179–184.
[55] K.C. Molloy, K. Quill, I.W. Nowell, J. Chem. Soc., Dalton Trans. (1987) 101–106.
[56] J. Styczynski, A. Kurylak, M. Wysocki, Anticancer Res. 25 (2005) 2253–2258.
[57] M. Ohno, T. Abe, J. Immunol. Methods 145 (1991) 199–203.
[58] M. Gielen, Coord. Chem. Rev. 151 (1996) 41–51.
[59] J.J. Bonire, S.P. Fricker, J. Inorg. Biochem. 83 (2001) 217–221.
[60] T. Higashi, A Program for Absorption Correction. Rigaku Corporation, Tokyo, Japan, 1995.
[61] G.M. Sheldrick, SHELXS-97, A Program for Automatic Solution of Crystal Structure. University of Goettingen, Germany, 1997.
[62] G.M. Sheldrick, Acta Crystallogr. Sect. A 64 (2008) 112–122.